GL01217

Preliminary Results of Hot Dry Rock Geothermal Heat Extraction Experiments at the Fenton Hill Site, New Mexico

May 1978

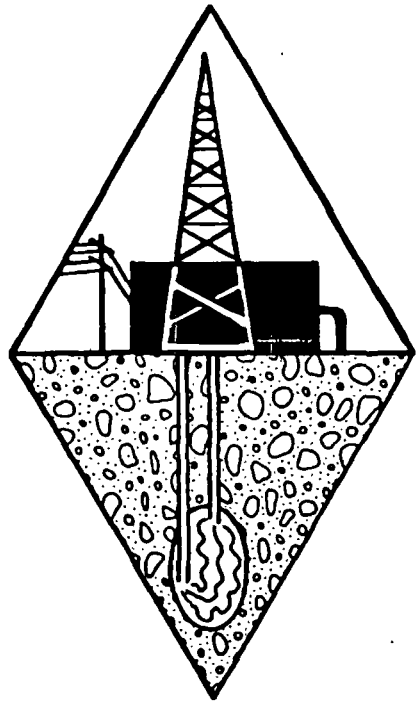

University of California

LOS ALAMOS SCIENTIFIC LABORATORY

Post Office Box 1663 Los Alamos, New Mexico 87545 505/667-5061

I. INTRODUCTION

On May 28, 1977, as the production well at Fenton Hill was being redrilled along a planned trajectory, it intersected a low-impedance hydraulic fracture in direct communication with the injection well, EE-1. Thus, a necessary prerequisite for a full-scale test of the LASL Hot Dry Rock Concept, that of establishing a high flow rate between wells at low wellhead differential pressures, was satisfied. Previously, communication with EE-1 had been through high-impedance fractures, and flow was insufficient to evaluate the heat-extraction concept.

In September, with much of the work on the surface plant of the energy-extraction loop nearly complete, we conducted a preliminary test of the entire system--surface plant and downhole flow paths. During 96 h of closed-loop circulation, fluid salinity remained low (<400 ppm), water losses continually decreased, and no induced seismic activity occurred. The operating power level was 3.2 MW (thermal) and fluid temperature reached 130°C at the surface. This test demonstrated for the first time that heat could be extracted at a usefully high rate from hot dry rock at depth and transported to the surface by a manmade system. The test further indicated a high probability that no significant problem would be encountered during sustained operation of the system.

Full-scale operation of the loop occurred from January 27 to April 12. During this Phase I test the thermal drawdown, impedance to flow, water losses, and fluid geochemistry of the system were studied in detail. In addition the experimental area was closely monitored for induced seismic activity. Results of these studies are briefly discussed.

II. LOOP OPERATION

During the Phase I operation, 20 channels of information about the loop were recorded: 7 flow rates, 8 pressures, and 5 temperatures. In addition to the loop instrumentation, 80 channels of thermocouple data were recorded. The thermocouples were strategically located on the heat exchanger to study possible corrosion and scaling problems.

Control functions for the Phase I loop were minimal. The CDA (Control and Data Acquisition) operator could manually start and stop four fans on the heat exchanger and manually stop the make-up pumps and main circulating pumps. A Hewlett Packard 9830 calculator was programmed to check all measurements against predetermined minimum and maximum values. If these parameters were exceeded the calculator would sound an alarm and define the problem with a printed statement. If the problem could result in damage to the pumps the calculator would also turn off all pumps immediately.

The numeric displays were updated every 15 s. All data channels were recorded on magnetic tape and on the line printer at 15-min intervals. If any of the predetermined parameters mentioned in the preceding paragraph was exceeded the recording interval changed to 1 min.

On January 27 the system was started by the make-up pump drawing water from the EE-1 fluid-reservoir pit. An output pressure of 175 psi was reached within a few minutes. At that time the main circulating pumps were turned on. The flow was into the EE-1 borehole, through the fracture system, and out of GT-2, where the flow was vented to the GT-2 pond. After several hundred thousand gallons of water had been pumped, the flow was diverted to the heat exchangers and back to the main pumps. The system was then "closed-loop." The inlet pressure to the main pumps was controlled by the make-up pump pressure, which in turn was controlled by a back-pressure valve. This valve was set at 175 psi and automatically diverted the make-up flow back to the EE-1 reserve pit when that pressure was exceeded. As the return flow from the heat exchanger gradually increased, the make-up flow was proportionally reduced. The EE-1 borehole pressure had been "red-lined" at 1300 psi for technical reasons. As the pressure approached that value, the flow was throttled at the control valve. After a few days the pressure and flow stabilized at ∿1300 psi and 125 gpm.

After 3 wk of operation in this mode, the impedance of the fracture system started to drop. The result was a demand for more flow to maintain the wellhead pressure. The control valve was therefore adjusted to allow for more flow. Finally the control valve was wide open, the flow exceeded 270 gpm, and the desired inlet pressure of 1300 psi could not be maintained. At that time we decided to control on flow, and a constant rate of 230 gpm was established.

The loop was operated under these conditions until it was "shut in" on April 13, 1978. "Shut in" was maintained for 10 days and then the system was vented.

The operation of the system for the 75 days of the test was an almost unqualified success. The system was "down" about 2% of the time. Equipment failures, largely a result of the use of new components and operation under winter conditions along with abrupt changes in flow rates through the downhole fracture system and interruptions in utility-supplied electrical power, necessitated only an occasional temporary cessation in circulation.

III. THE DOWNHOLE SYSTEM

Figure 1 summarizes the current knowledge of the distribution of the flow between wells. About 90% of the water pumped into EE-1 is injected into a single fracture at 9030 ft, where the temperature of undisturbed rock is 185°C. The fracture at that depth is believed to be a member of a series of ancient northwesterly striking vertical fractures separated horizontally by distances of 15 to 20 ft, which have been hydraulically reopened. Flow into any fractures intersected above the main injection point is blocked by casing cement. Below this point fractures have high intrinsic impedances at current operating pressures. Flow through the 9030-ft fracture enters the producing well through four fractures intersecting GT-2B, but two fractures (one at 8755 and the other at 8860 ft) account for most of the flow. The fractures intersecting GT-2B must be considered distinct from the main fracture in EE-1. Not part of the northwesterly striking set, they intersect the main fracture and provide for the lateral flow which is necessary to complete the connection between wells.

IV. THERMAL POWER AND DRAWDOWN

Injection and production flow rates were measured with venturi meters and differential-pressure transducers. Surface injection and production temperatures were measured with thermocouples inserted into the wellheads. In addition, a temperature-surveying tool employing a thermistor was positioned downhole in the production well, designated as GT-2B, for almost the entire duration of the test. A total of 58 surveys was run during Phase I heat production. Between surveys the tool was stationed at 2.6 km (8600 ft),

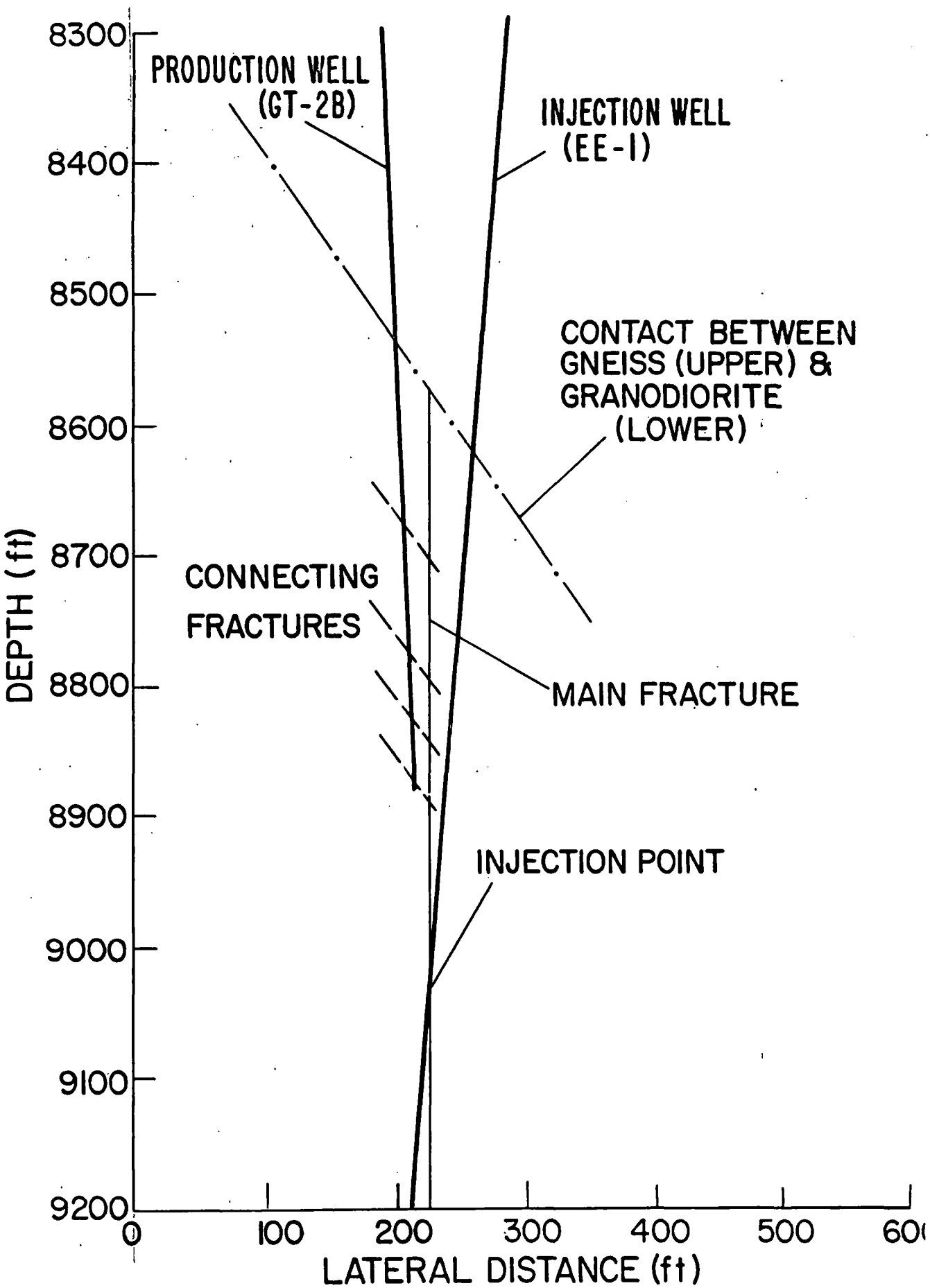

Figure 1. The inferred fracture system in relation to Fenton Hill injection and production wells (NE-SW) section.

just downstream (that is, uphole) of all the known flow connections between the reservoir and the production well. In this fashion the mixed-mean temperature of all the water flows converging on GT-2B was almost continuously monitored. Typical surveys are presented in Fig. 2. The uppermost survey was obtained on February 4, 1978, 7 days after the start of power production, while the middle and lower surveys were obtained after 12 and 16 days, respectively. Even a cursory look at these surveys indicates a reservoir-to-well connection of fascinating complexity. The major temperature changes at the depths indicated are associated with flow connections that had been identified in earlier testing. (The uppermost connection was actually identified upon re-examining the earlier data.) We found in earlier testing that 20% and 80% of the flow entered the production well through the deepest and next-deepest of these four connections, respectively, while the flow rates in the upper two were too small to be measured. Both major connections 1 and 2 actually consist of two connections each. At connection 2, a definitely colder flow entered at the bottom while 2 m up, water at least 5° hotter entered the well. The February 9 survey, and even more pronouncedly the February 13 survey, show the development of new flow connections between the previously determined major connections 1 and 2; and, in fact, the magnitude of the temperature change at 2.68 km (8800 ft) suggests that a major new connection has also developed there. Unlike the injection well, which operates at high pressure, the pressure in the production well is close to normal hydrostatic, so we conclude that this new connection was caused by thermal or chemical-dissolution effects rather than by pressurization.

Figure 3 presents the variation of temperature at 2.6 km (8500 ft) with time. This represents the best indication of the overall thermal drawdown of the reservoir. Also shown are theoretical results for a reservoir with a surface area (one side only) of 8000 m^2 (8.6 x 10^4 ft^2). In the computation, the fracture aperture was assumed to be constant, 0.2 mm; the assumed inlet temperature was 50°C; the inlet was located 30 m above the fracture bottom; and the outlet was located at the top. We assumed that in addition to the GT-2 outflow, one-half of the make-up flow was effectively extracting heat. The temporal variation of this combined flow rate was represented as a curve with three linear segments. The "scallop" in the predicted and measured temperatures at 25 days is due to a rapid flow-rate increase.

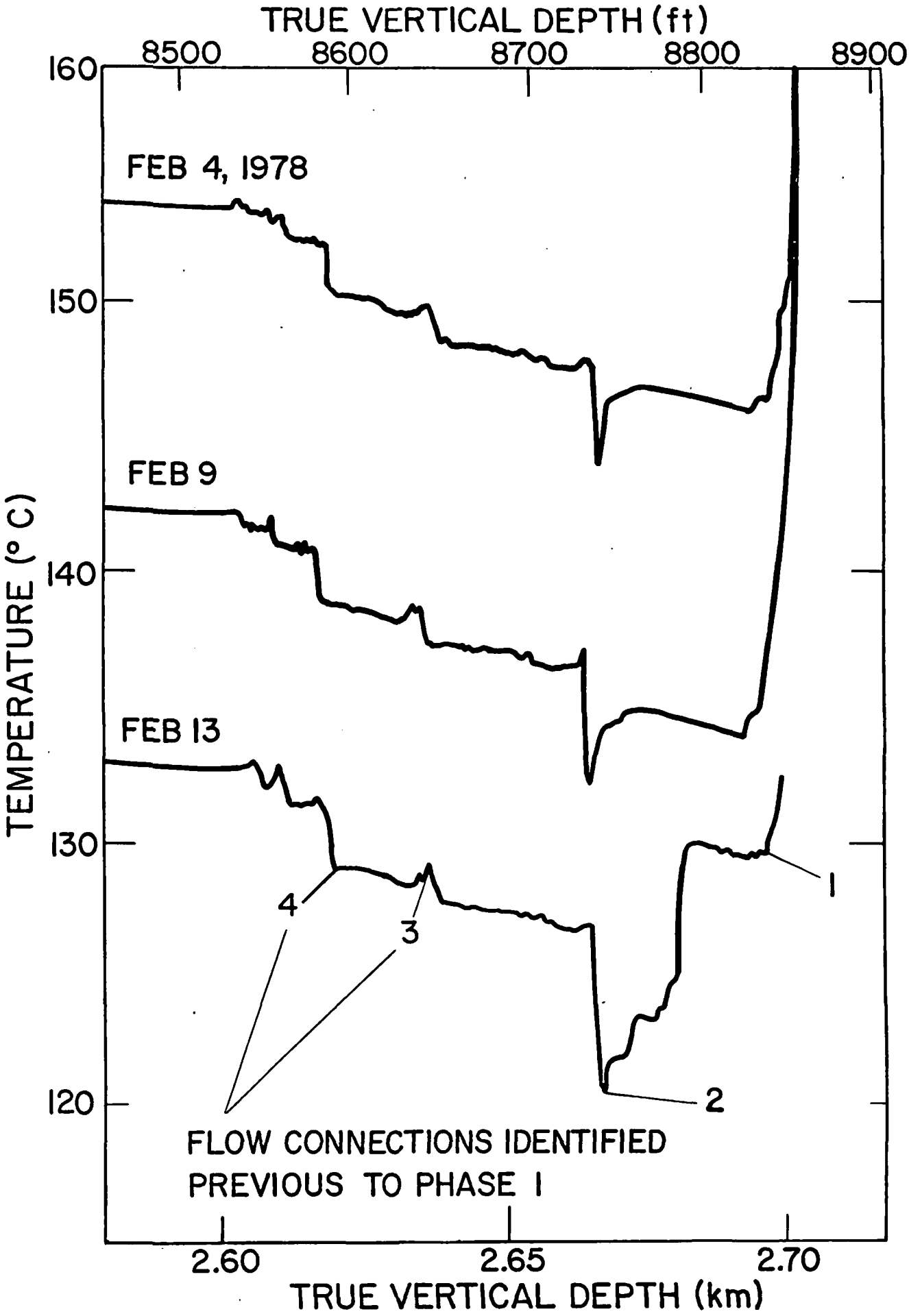

Figure 2. Temperature surveys in production well GT-2B.

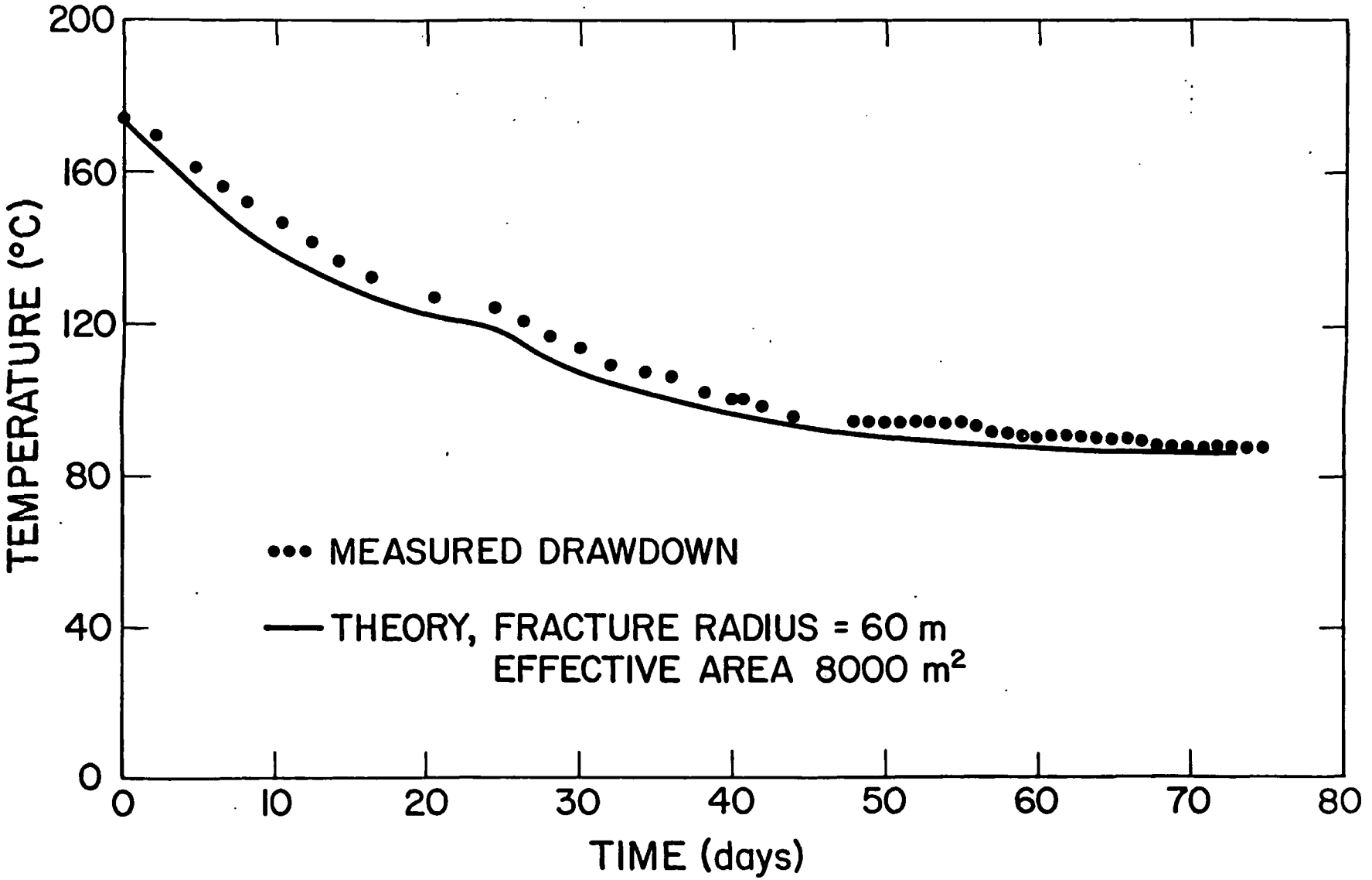

Figure 3. Reservoir production temperature.

The theoretical curve indicates that the downhole temperature always decreases, but at a slower and slower rate; in contrast, the data on several occasions have shown absolutely no decrease for periods as long as several days. Thermal-stress cracking, if it did occur, occurred so late in this phase of the test that it has not so far contributed much to thermal performance. In fact, even if the temperature were to remain perfectly steady for 20 days (a rather unlikely event), the actual temperature would still be only a few degrees higher than that predicted. Given the relatively short time scale for the test, the only reasonable way to convincingly demonstrate thermal-stress cracking would have been to increase the flow rate considerably so as to drive the predicted curve downward, and then to see if the actual temperature followed the prediction.

Because of the decreasing impedance, the flow rate could not be maintained at constant pressure for long periods at more than ∿230 gpm. Consequently, the energy extraction rate increased gradually to ∿5 MW (t) as flow rate increased to ∿270 gpm, and thereafter remained nearly constant at ∿4.3 MW (t) while flow rate was reduced for safety considerations to 230 gpm (Fig. 4). The effects of temperature drawdown on energy extraction rate were obscured by these changes in flow rate.

V. FLOW IMPEDANCE

Flow impedance is the pressure drop through the fracture system connecting the two wellbores divided by the flow rate. There is some ambiguity in this definition because the inlet flow differs from the outlet flow by the rate at which water diffuses into the rock surrounding the fracture. Conservatively, one may use the outlet flow rate in calculating impedance. Because there were no downhole pressure gauges, the downhole pressure drop through the fracture system was obtained from the pressure difference between EE-1 and GT-2 measured at the surface and corrected for the difference in density of water in the two wellbores.

In the course of this test, the impedance began to fall after 1 wk of flow. Figure 5 is an idealized (averaged) graph of the flow and pressure history in EE-1. After attaining a roughly constant value of 15 psi/gpm in the first few hours of operation the flow rate into EE-1 was limited by surface plumbing and, as the impedance dropped and it became impossible to hold constant

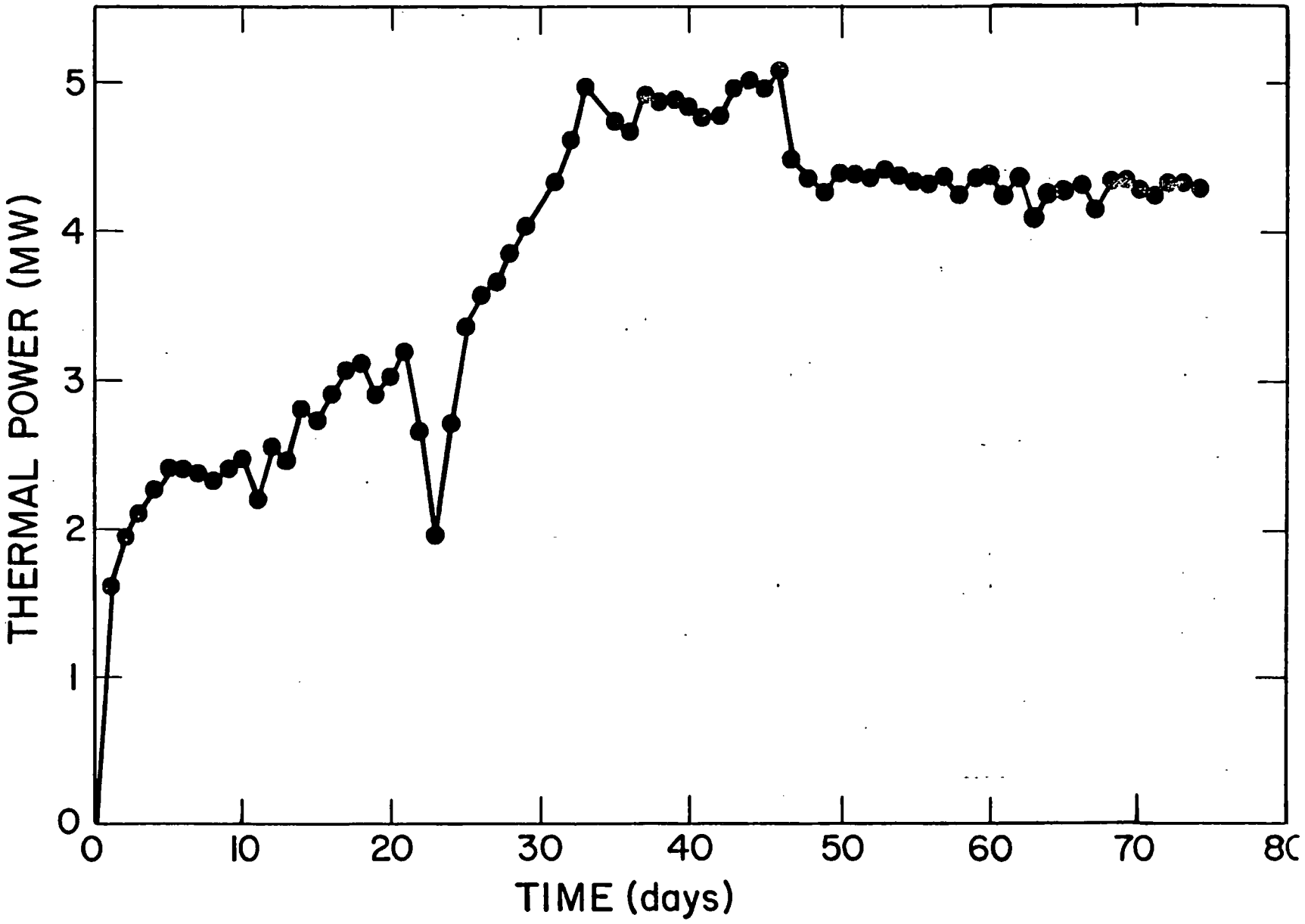

Figure 4. Thermal power variation.

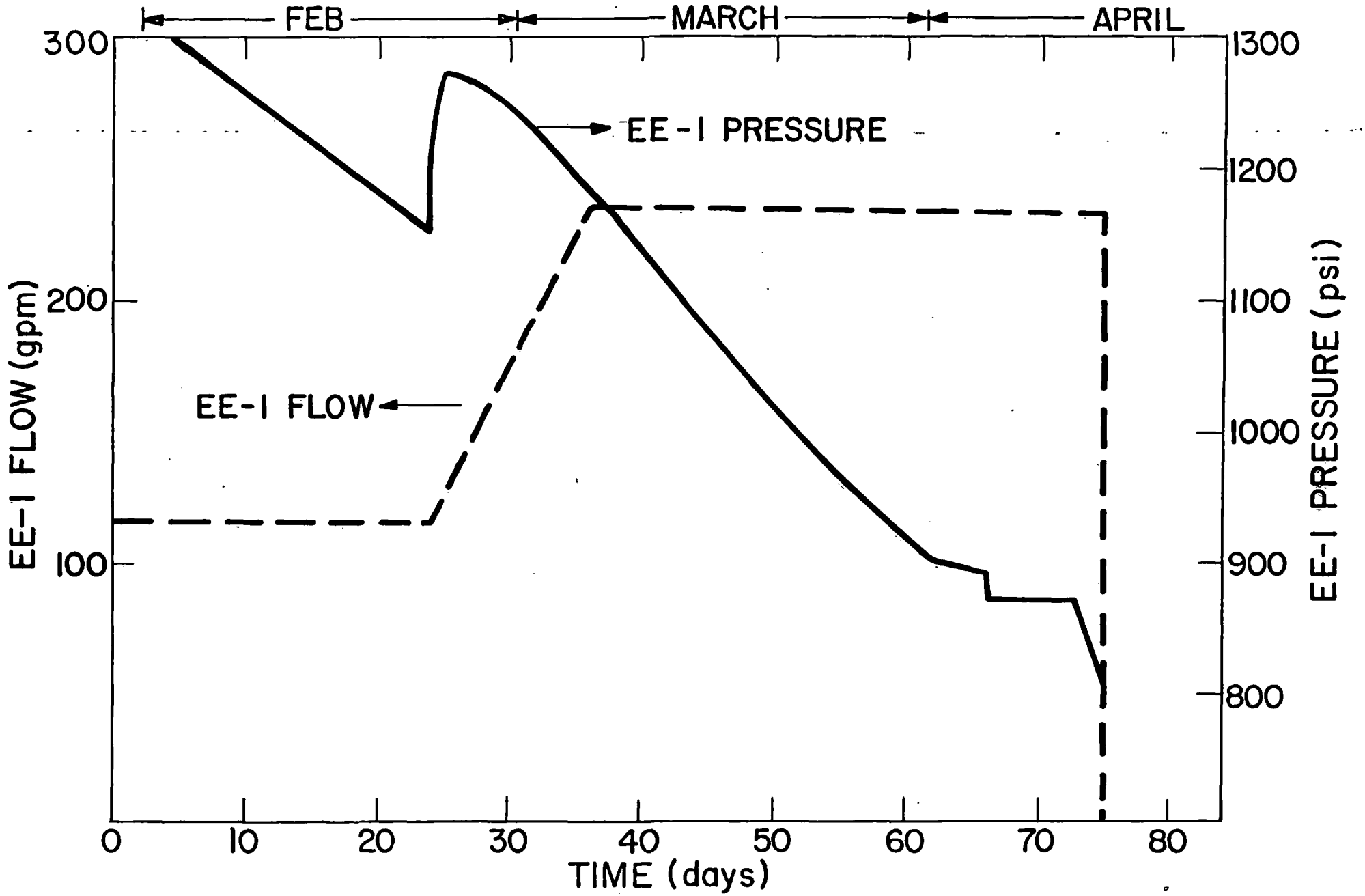

Figure 5. Idealized pressure and flow history in EE-1.

pressure, it was decided to maintain constant flow rate. This was done during the second half of the test, as seen in Fig. 5.

The impedance decreased to less than 1/3 of the original value in the first 40 days, but decreased only 25% more from day 40 to the end of the run at day 75. This is shown in Fig. 6. Throughout the 75-day period, numerous discontinuous decreases in impedance occurred, contributing to the overall decrease. None was associated with seismic effects observable at the surface.*

Continuous changes in impedance may have been the result of the shrinkage of fracture faces away from each other, caused by cooling and pressurization. Abrupt changes in impedance may have resulted from changes in the compressive stresses within the reservoir, caused by cooling or pressurization of the entire region. When the stresses in the rock decrease together, so that the stress differences do not change, the normal stresses across many of the fractures will decrease while the shear stress remains constant, and one fracture face may slip across the other. Because the pre-existing fractures were not truly planar, this slippage may result in a partially open crack, supported by small irregularities along the faces. Such an event would represent an abrupt change in flow impedance.

The real reservoir must be much more complex than any of these models, with both irregular regions of cooling and irregular regions of pressurization (not necessarily the same regions). Stresses will be relieved in some regions and concentrated in others, possibly leading to extensive breaking up of the rock.

VI. WATER LOSSES

During the test a total of 18 million gallons of water flowed between the wells through the fracture system. Of this, 1.3 million gallons were lost to the surroundings. Since the termination of closed-circuit flow, 300 000 gal or roughly 1/4 of this has returned through GT-2B. Figure 7 shows the water losses expressed in terms of flow rate. Water-loss rate decreased from

*Many small impedance decreases must have been missed, but those which were observed were sufficient to account for over half of the flow increase observed during the run. Thus, many of the events which gave rise to impedance changes took place within a short time span, possibly only fractions of a second.

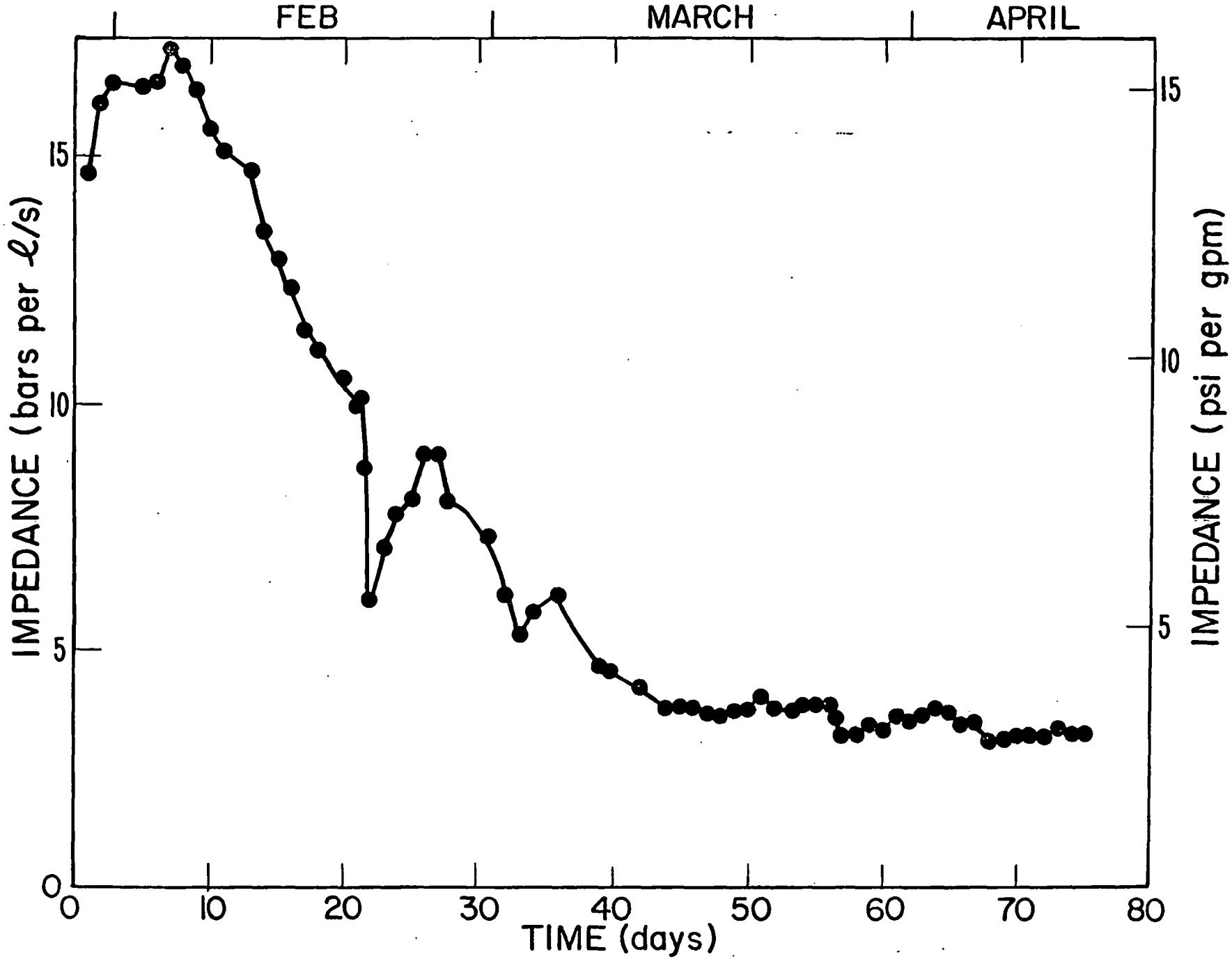

Figure 6. Flow impedance.

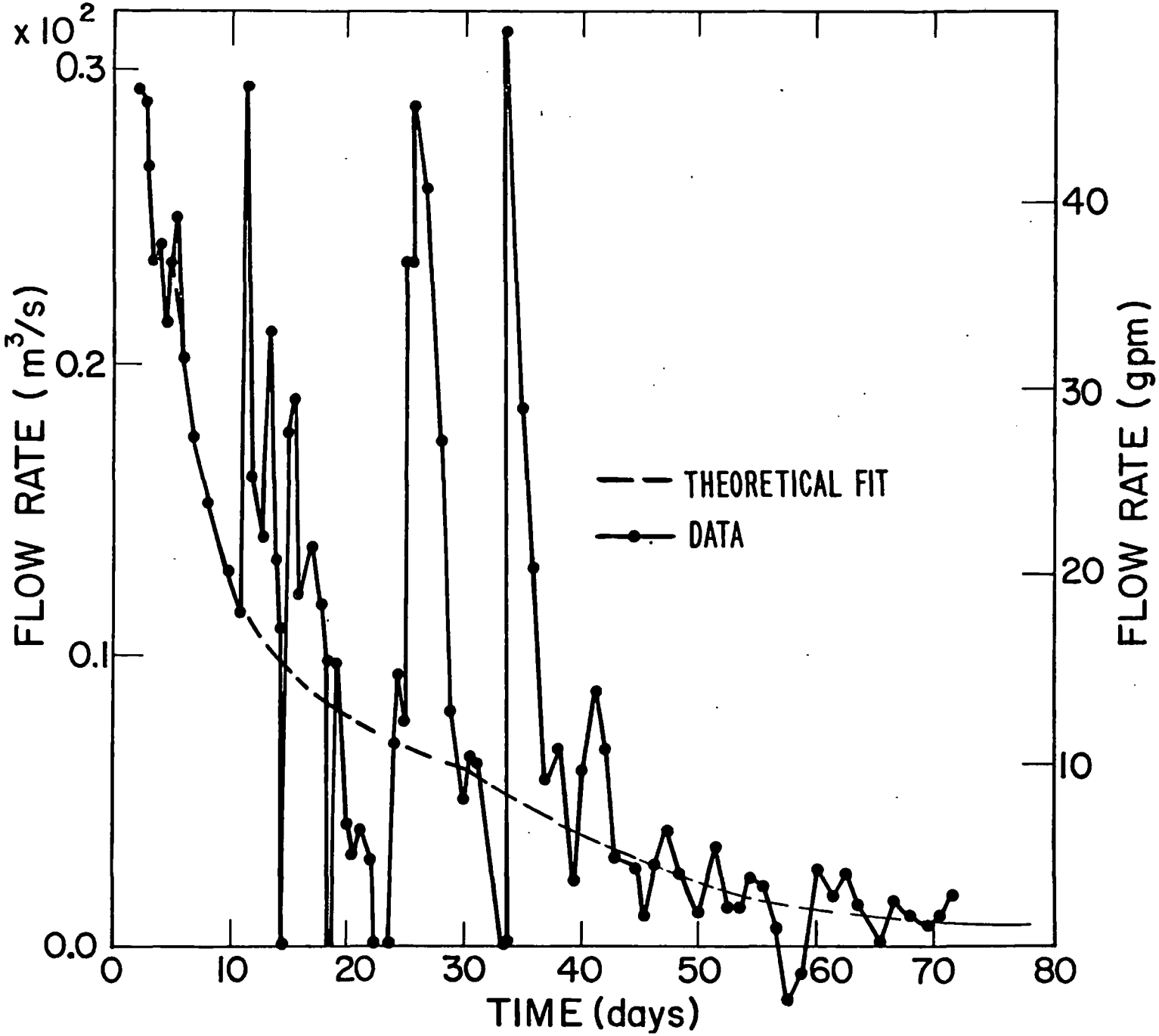

Figure 7. Water loss.

a high in excess of 2.5 ℓ/s (40 gpm) to 0.6 ℓ/s (10 gpm) after 25 days of flow at a system throughput flow rate of 7.5 ℓ/s (120 gpm). Subsequently, as the flow rate was increased to the peak sustained flow of 14.5 ℓ/s (230 gpm), water losses dropped to less than 0.3 ℓ/s (5 gpm), or 1-1/2% of throughput flow.

The dashed line of the figure is the result from a two-dimensional computer model. This is a nonlinear diffusion model describing the permeation of the water into the pores and fractures in the surrounding rock. For this calculation the input was the measured pressure that drives the water into the surrounding rock, that is, the pressure in the EE-1 wellbore corrected to the bottomhole value. The many short-term transients are caused by operational shut downs and are included in the calculations. The general trends, however, are as expected for this type of water-loss phenomenon. For a nearly constant pressure from the first to the 25th day the loss rate decreased as the porosity near the main fracture was filled with water and pressurized. After 25 days the decrease continued, but at a faster rate in response to a decreasing pressure in the EE-1 wellbore. The data of Fig. 8 are the integral of the water loss as recorded independently on a totalizing flow meter, and are corrected for the major vent that occurred on the 23rd day. The solid curve of this figure is the result of the same calculations that are plotted on the previous figure. Because the short-term transients are not obvious in the integral data, the general agreement with the diffusion calculations can be seen. The general trends in the data and the diffusion model indicate that the water-loss rate would have decreased to even lower values if the experiment had continued.

VII. WATER CHEMISTRY

Analyses were made throughout the test for the following dissolved species: Ca, Na, K, Si, F, SiO_2, Cl, and SO_4. In addition, the conductivity and pH of the water were measured. Representative curves of concentration versus time are given in Figs. 9 and 10. The variation in conductivity is given in Fig. 11. There are several features common to all of the graphs. First, the very early samples had high concentrations of each of the species measured, and due to dilution with make-up water, these high concentrations dropped very rapidly. These early samples reflect the nature of the water, which had been

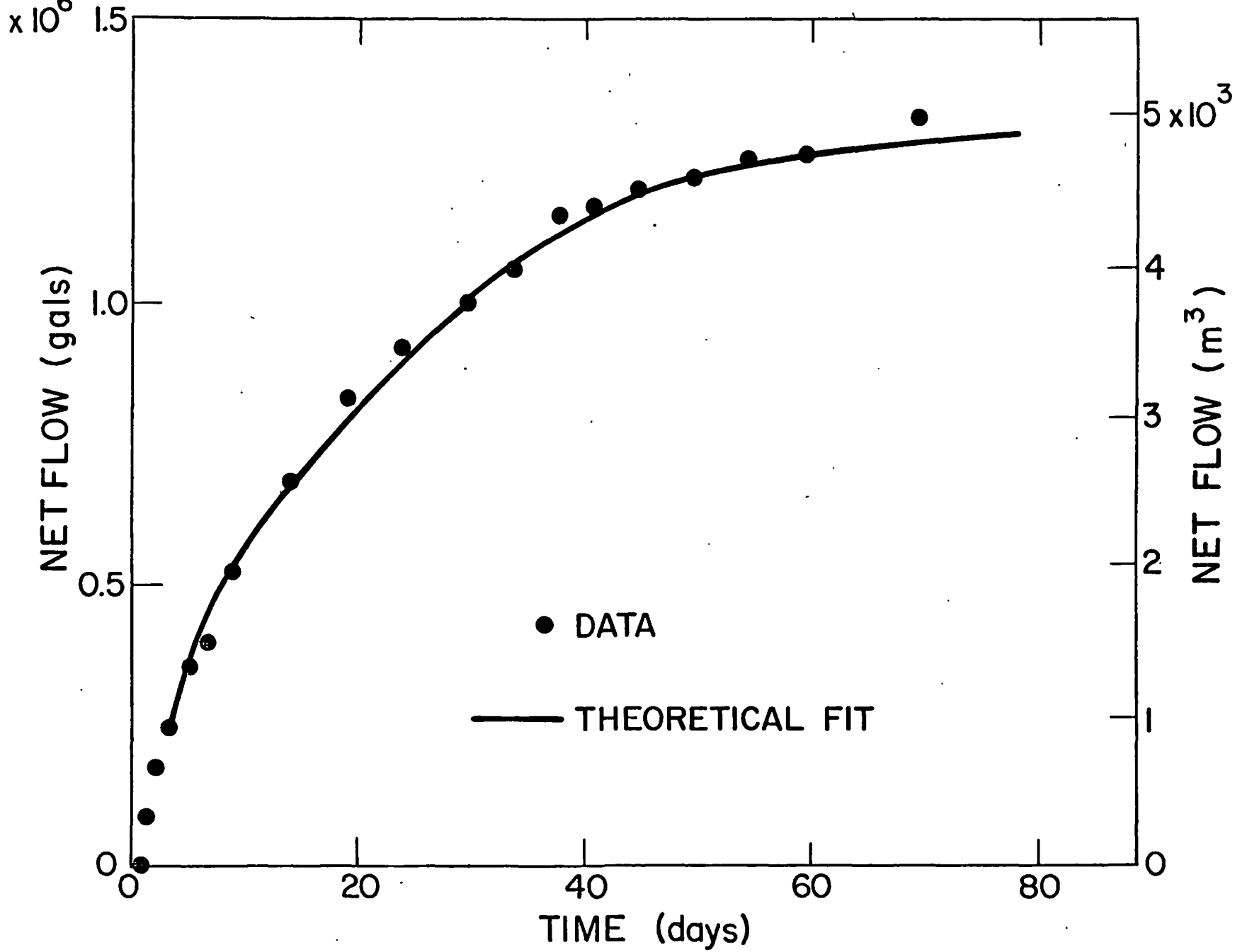

Figure 8. Net water loss.

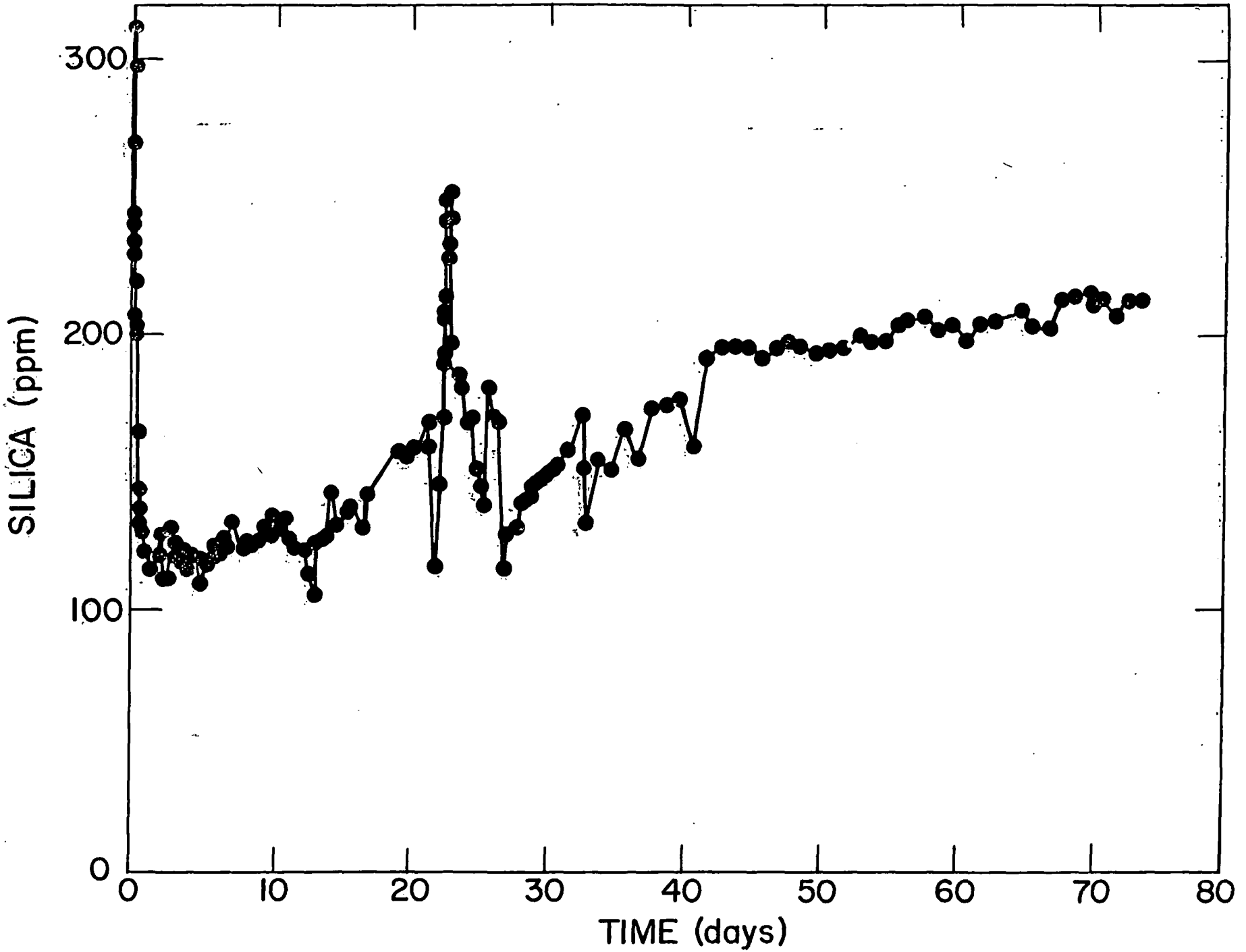

Figure 9. Silica concentration versus time.

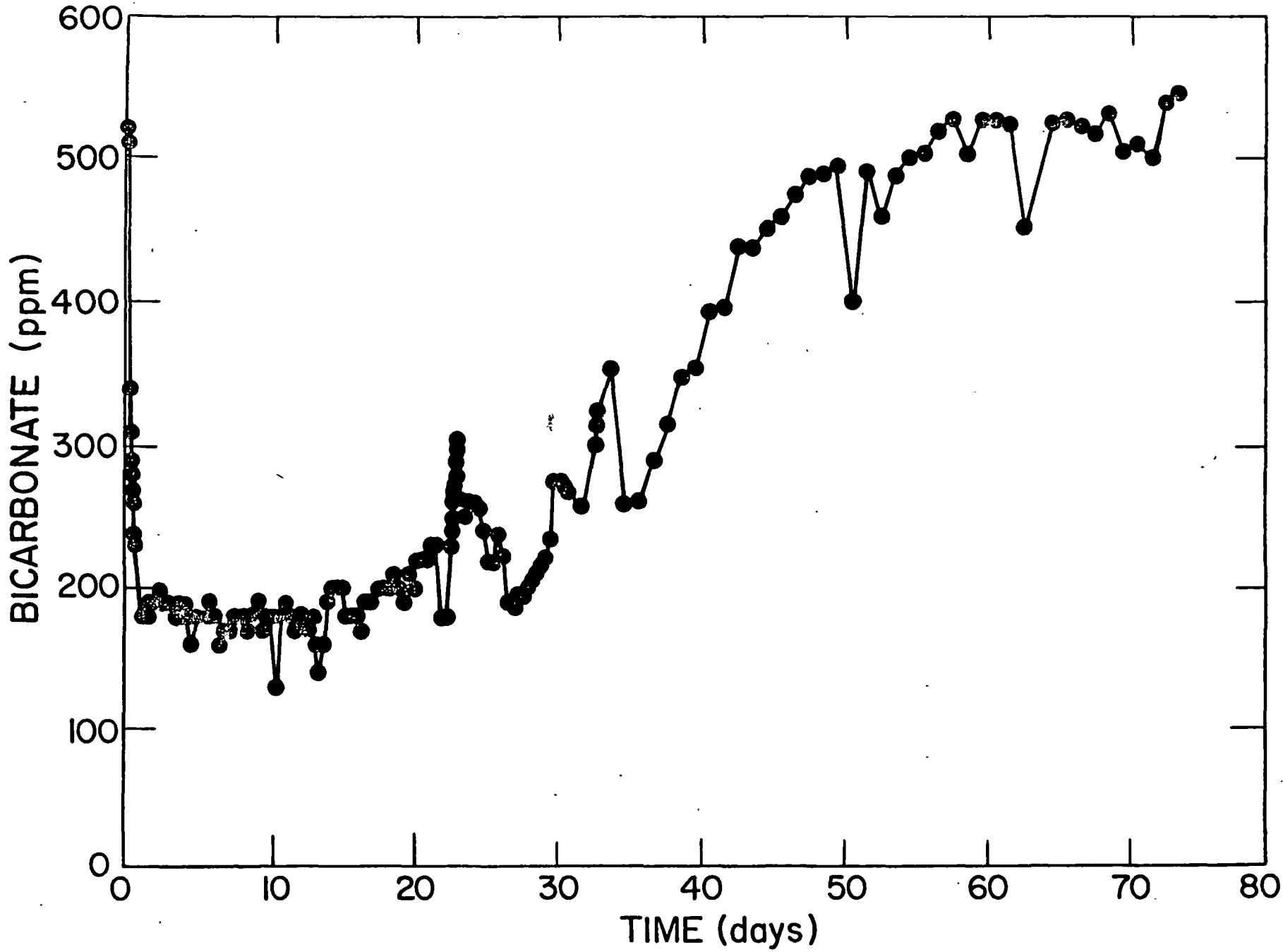

Figure 10. Bicarbonate concentration versus time.

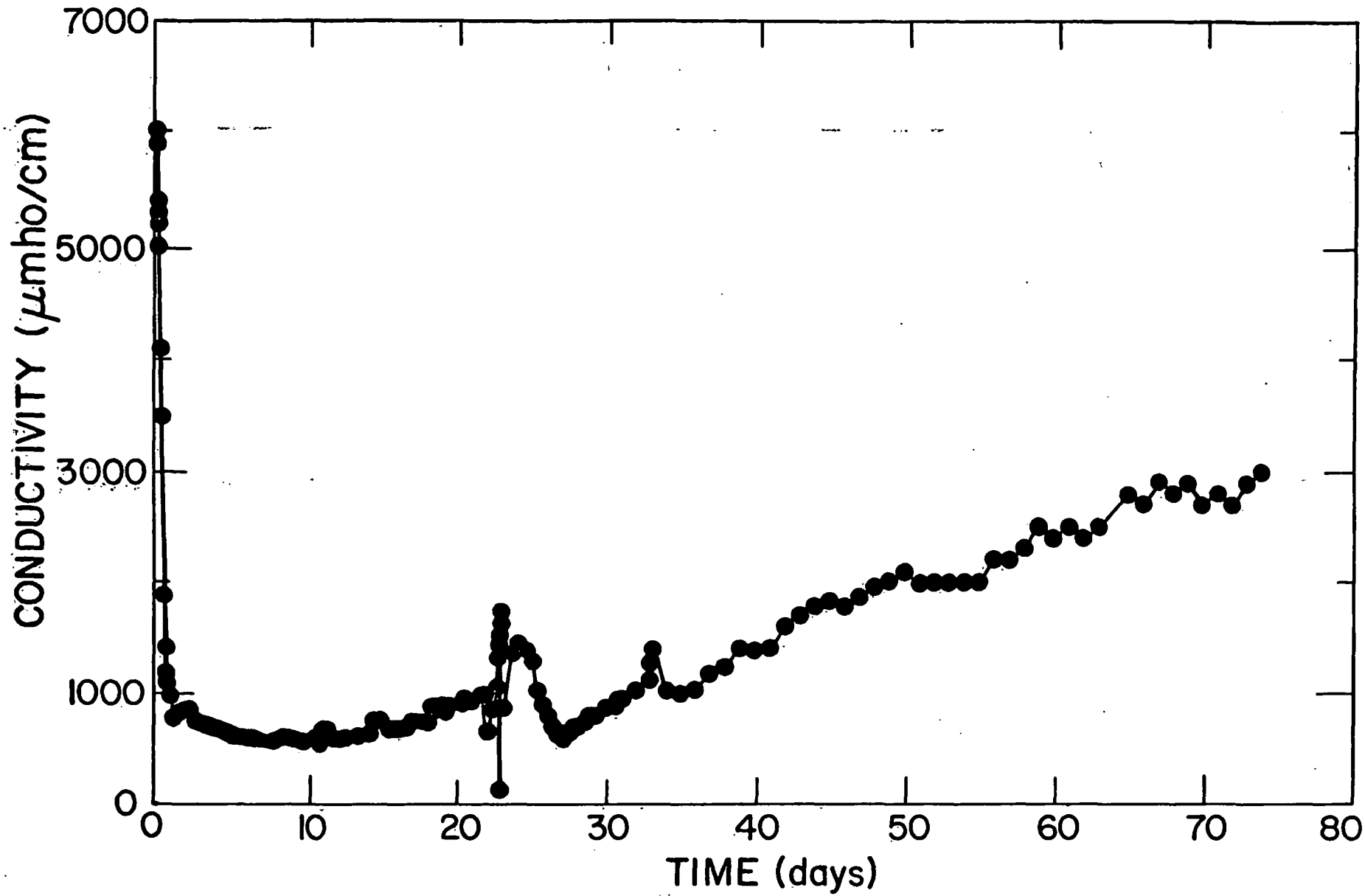

Figure 11. Fluid electrical conductivity.

stagnant in the reservoir for more than 3 months. After an initial flushing of the reservoir (∿60 000 gal) in which the water recovered at GT-2 was discarded, the system was operated as a closed loop and the make-up flow rate equalled the water losses to permeability storage in the reservoir. As the make-up requirements dropped, the dilution effect was lessened and the concentrations of dissolved material began to rise toward "saturation" values. On several occasions, the system had to be shut down for various lengths of time. The effects of shut-downs are apparent in the chemistry of the fluids. As the pressure in the system dropped, water which had been stored in the rock returned to the reservoir and then to the surface, carrying more dissolved material because of longer periods of contact with the rock and higher rock temperatures. The spike on each graph at day 23 is an example. As the system was restored to operating temperatures and pressures, make-up losses were again high to replace fluid which had returned from the permeability storage. This high make-up had a strong dilution effect as is seen in the "low" just after the 23rd day.

Dissolution of minerals continued until the end of the run. Several curves show an apparent leveling off starting at days 40 - 50. Notwithstanding the general increase in the salinity of the water, in absolute terms the concentration of dissolved solids remained low. Visual inspection of the interior of the major flow line indicated no apparent deposition or corrosion. Some deposition of calcite did occur at sample ports and at points along the lines where leaks had occurred. Silica concentrations exceeded the quartz saturation value at the measured temperature of the fluid leaving the reservoir.

VIII. SEISMIC MONITORING

Seismic monitoring was done to detect local seismic sources and to discriminate among several possible source types -- manmade disturbances, earthquakes, and faulting induced by the pressurized fluid injection into the inlet well of the HDR system.

The monitoring array consisted of seven surface stations at distances up to 750 m from the wells, two shallow borehole stations (∿125-m deep) at about 1 and 3 km, and stations of the LASL regional seismic network -- the nearest of which is about 10 km away. The two borehole stations were positioned a few meters below the Permian sandstone -- Quaternary tuff interface.

The only local earthquakes identified during the loop operation were located by the array near a fault 15 km west of the HDR geothermal site. These microquakes had local magnitudes (M_L) of -0.8, 0.0, and 0.5 as determined by signal duration. Many blasts and earthquakes were observed with more distant epicenters, and many sonic booms. Some of the smaller of these acoustic signals required the seismograms of the regional network for positive identification.

The background noise at the Fenton Hill site was generally high during the day, beginning with sunrise when thermal expansion of the metal sheds took place, and the amplitudes of noise bursts frequently exceeded levels expected for M_L = 1.0 earthquakes. At night, however, the background noise was nearly always below signal levels for M_L =-1.0 earthquakes.

Although it is likely that $M_L < 0.0$ earthquakes would not have been identified during the daytime, the absence of detected induced earthquakes with $M_L > -1.0$ at night is reasonable evidence that none with $M_L > 0.0$ occurred during the loop operation.

IX. SUMMARY

- The surface facilities and data acquisition systems proved sufficient for a short-term test (75 days) of the first artificially produced geothermal reservoir.
- Thermal drawdown for the first small experimental system followed closely the theoretical curve for an 8000-m^2 system.
- Reservoir flow impedance decreased from an initial 1625 KPa-s/ℓ (15 psi/gpm) to about 325 KPa-s/ℓ (3 psi/gpm) by both continuous and discontinuous drops in impedance.
- Permeation water-loss rate quickly decreased to less than 3 gpm (<1-1/2% of circulation rate).
- Geofluid chemistry is most acceptable, with 1500 - 2000 ppm total dissolved solids and no evidence of scaling in main flow passages.
- There is no evidence of any measurable seismicity induced at the site.